



Wind Turbine Noise Modelling Based on Amiet's Theory

Yuan Tian, Benjamin Cotté, Antoine Chaigne

► **To cite this version:**

Yuan Tian, Benjamin Cotté, Antoine Chaigne. Wind Turbine Noise Modelling Based on Amiet's Theory. 5th International Meeting on Wind Turbine Noise, Aug 2013, Denver, CO, United States. CD-ROM proceedings. hal-00975237

HAL Id: hal-00975237

<https://hal-ensta-paris.archives-ouvertes.fr//hal-00975237>

Submitted on 8 Apr 2014

HAL is a multi-disciplinary open access archive for the deposit and dissemination of scientific research documents, whether they are published or not. The documents may come from teaching and research institutions in France or abroad, or from public or private research centers.

L'archive ouverte pluridisciplinaire **HAL**, est destinée au dépôt et à la diffusion de documents scientifiques de niveau recherche, publiés ou non, émanant des établissements d'enseignement et de recherche français ou étrangers, des laboratoires publics ou privés.

**5th International Meeting
on
Wind Turbine Noise
Denver 28 – 30 August 2013**

Wind Turbine Noise Modelling Based on Amiet's Theory

Y. Tian ENSTA ParisTech, 828, boulevard des Maréchaux, 91762 Palaiseau Cedex, France tian@ensta.fr

B. Cotté benjamin.cotte@ensta.fr

A. Chaigne antoine.chaigne@ensta.fr

Summary

Broadband noise generated aerodynamically is the dominant noise source for a modern wind turbine (Brooks *et al*, 1989; Oerlemans *et al*, 2007). In this paper, two main broadband noise mechanisms, namely trailing edge noise and turbulent inflow noise, are examined in detail using frequency domain noise prediction models based on Amiet's analytical theory. Improvements are proposed to adapt the original model to wind turbines. First, a wall pressure spectral model proposed recently by Rozenberg, Robert and Moreau that considers an adverse pressure gradient flow (APG) is applied to the trailing edge noise model. This APG model leads to a significant increase in the sound pressure level. Second, an empirical airfoil thickness correction is proposed in the turbulent inflow noise model, which introduces a level reduction that depends on leading-edge thickness, frequency and the ratio of the turbulence integral length scale to the blade chord. The proposed model also includes Doppler effect for rotating blades. Calculation results are validated by comparison with wind tunnel experimental data and with measurements for a full size wind turbine. This model is also used to quantify the amplitude modulation that can be a source of annoyance in the vicinity of a wind farm.

1. Introduction

Nowadays, wind energy application grows rapidly as a renewable, clean energy. While profiting from wind energy, the noise produced by a modern wind turbine becomes a main problem for the neighbourhood of a wind farm. The annoyance due to amplitude modulation (swish) and to the low frequency noise is especially a concern for the people living close to a wind farm (Styles *et al*, 2011).

Two main noise sources from modern wind turbines are turbulent inflow noise and trailing edge noise (Oerlemans *et al*, 2007). The former is induced by the scattering of atmospheric turbulence fluctuation at the leading edge of the blade, sometimes referred to as the leading edge noise; the latter is due to the turbulent boundary layer passing by a sharp edge like the trailing edge. Both noise mechanisms are broadband, and depend on the wind turbine size and on the atmospheric turbulence conditions; the total noise level can be dominated by one or the other.

The goal of this paper is to propose a theoretical noise prediction model, that can be used to study different phenomena related to wind turbine noise (amplitude modulation, wind shear effects, etc). The model is also intended to be coupled to an atmospheric propagation model for the prediction of the far field sound pressure level (SPL). In this paper, a well known analytical model proposed by Amiet (1975, 1976) is chosen for the noise prediction. The original model is based on a flat plate with semi-infinite chord. As an improvement, an empirical correction on airfoil thickness for turbulent inflow noise is applied. Results show that increasing airfoil reduces the turbulent inflow noise. Furthermore, a wall pressure spectra model proposed by Rozenberg *et al*. (2012), which considers an adverse pressure gradient (APG) flow is validated and applied to Amiet's trailing edge noise model. This wall pressure model will increase the sound pressure

level to a certain level that depends on the flow conditions. The paper is organized as follows: in section 2, a brief introduction to the Amiet's analytical model is given; in section 3, two main improvements, namely, airfoil leading edge thickness and the APG model for the trailing edge noise are explained in detail; section 4 shows the validation for the improved models against the measurements of fixed airfoils; section 5 contains the results from a real size wind turbine calculation validated against the measurements; the conclusions and acknowledgements are in section 6.

2. Amiet's Analytical model for turbulent inflow noise and trailing edge noise

In this section, Amiet's analytical models for both noise mechanisms are briefly introduced. Section 2.1 is devoted to turbulent inflow noise and section 2.2 to trailing edge noise.

2.1. Amiet's model for turbulent inflow noise

An airfoil in a turbulent flow experiences a fluctuation lift loading (unsteady upwash) which will result in the generation of sound. Considering the complex nature of turbulence and its interaction with the airfoil, many previous researchers proposed their models based on some common assumptions (Howe, 1978): 1. the incoming turbulence fluctuation is considered to be small compared to the mean flow velocity; 2. the interaction between an airfoil and the turbulent flow is inviscid so that the problem is reduced to solving linearized Euler equations. In Amiet's model (Amiet, 1975), the turbulent gust properties are assumed unchanged while it is convected by the mean flow, and its velocity fluctuation is represented in terms of chord-wise and span-wise wave number, here, K_x and K_y respectively, (see Figure 1). The airfoil is modelled as a flat plate with no thickness, where the chord is c and the span is L . The model further assumes that the plate has semi-infinite chord and infinite span extension.

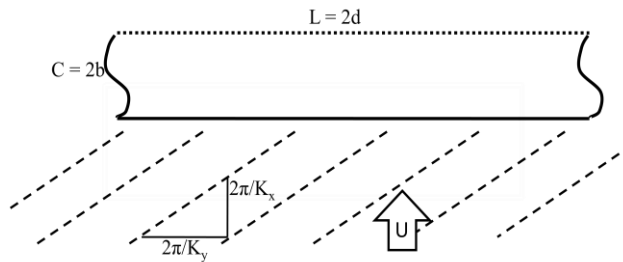


Fig.1 Geometry and notations used in the turbulent inflow noise model.

If we write the incident gust in the Fourier domain in the form as:

$$w = w_0 e^{i(\omega t - K_x x - K_y y)}, \quad (1)$$

then the fluctuating velocity field is deduced as:

$$\phi(x, y, z, t) = \phi(x, z) e^{i\omega t} e^{ikM/\beta^2 x} e^{-iK_y y}, \quad (2)$$

where $\phi(x, y, z, t)$ is the velocity potential and M is the Mach number, $\beta^2 = 1 - M^2$. Substituting Equation (2) into the convective wave equation we obtain:

$$\frac{\partial^2 \phi}{\partial \bar{x}^2} + \frac{\partial^2 \phi}{\partial \bar{z}^2} + \bar{k}^2 \phi = 0,$$

where

$$\bar{x} = \frac{x}{b}, \quad \bar{y} = \frac{y}{b}, \quad \bar{z} = \frac{z}{b}, \quad \bar{K}_x = bK_x, \quad \bar{K}_y = bK_y, \quad \bar{k} = bk,$$

b is half chord, k is the acoustic wave number, and

$$\bar{\mu} = \bar{K}_x M / \beta^2, \quad \bar{k}^2 = \bar{\mu}^2 - \bar{K}_y^2 / \beta^2,$$

with U the free stream velocity. Solving for ϕ and using the relationship between acoustic pressure and velocity potential, we can finally get the pressure fluctuating on the airfoil surface as (Rozenberg, 2007):

$$p(x, y, 0, t) = \rho_0 w_0 U \frac{e^{-i\pi/4}}{\sqrt{\pi(\beta^2 \bar{\kappa} + bK_x) \frac{x}{b}}} e^{i\omega t - ix(K_x - A/b) - iK_y y}, \quad (3)$$

with $A = -kM/\beta^2$.

Assuming that the source behaves like a dipole source, and applying Lighthill analogy, the power spectrum density of far field acoustic pressure is obtained from Equation (3) as (Amiet, 1975; Rozenberg 2007):

$$S_{pp}(\vec{x}, \omega) = \left(\frac{\rho_0 \omega c x_3}{2c_0 S_0^2} \right)^2 U \int_{-\infty}^{\infty} \Phi_{ww} \left(\frac{\omega}{U}, K_y \right) \mathcal{L}^2 \left(x_1, \frac{\omega}{U}, K_y \right) \text{sinc}^2 \left[\frac{L}{2} \left(\frac{kx_2}{S_0} - K_y \right) \right] dK_y, \quad (4)$$

where ρ_0 is the air density, and c_0 is the sound velocity. $\vec{x} = (x_1, x_2, x_3)$ is the observer coordinate, \mathcal{L} is the airfoil response function, $\text{sinc}^2(x) = \frac{\sin^2(x)}{x^2}$, S_0 is a modified distance between the source and observer. Φ_{ww} is the turbulence energy spectrum. If we assume a infinite span, $L \rightarrow \infty$, the $\text{sinc}^2(x)$ function could be evaluated by a Dirac function, and thus Equation (4) reduces to:

$$S_{pp}(\vec{x}, \omega) = \left(\frac{\rho_0 \omega c x_3}{2c_0 S_0^2} \right)^2 \pi U \frac{L}{2} \Phi_{ww} \left(\frac{\omega}{U}, \frac{kx_2}{S_0} \right) \mathcal{L}^2 \left(x_1, \frac{\omega}{U}, \frac{kx_2}{S_0} \right). \quad (5)$$

Equation (5) is referred to as the simplified equation under large aspect ratio assumption.

2.2 Amiet's model for trailing edge noise

Trailing edge noise is generated by the scattering of the turbulent boundary layer passing by the trailing edge. Since the origin is the fluctuation of turbulent boundary layer, the derivation is similar to that of turbulent inflow noise, here only the final result, the power spectrum density of far field sound is cited as (Amiet, 1976; Roger *et al.* 2005):

$$S_{pp}(\vec{x}, \omega) = \left(\frac{\omega L x_3}{4\pi c_0 S_0^2} \right)^2 \frac{c}{2\pi} \int_{-\infty}^{\infty} \Phi_{pp}(\omega) \ell_y(\omega) \mathcal{L}^2 \left(\frac{\omega}{U}, K_y \right) \text{sinc}^2 \left[\frac{L}{2} \left(\frac{kx_2}{S_0} - K_y \right) \right] dK_y, \quad (6)$$

$$S_{pp}(\vec{x}, \omega) = \left(\frac{\omega c x_3}{4\pi c_0 S_0^2} \right)^2 \frac{L}{2} \Phi_{pp}(\omega) \ell_y(\omega) \mathcal{L}^2 \left(\frac{\omega}{U}, K_y \right) \quad (7)$$

which are the exact formula and simplified formula under large aspect ratio assumption respectively. $\Phi_{pp}(\omega)$ is the power spectral density of wall pressure, and $\ell_y(\omega)$ is the span-wise correlation length.

3. Model improvement: adverse pressure gradient wall pressure model and leading edge thickness correction

3.1 Airfoil thickness correction for turbulent inflow noise

Roger and Moreau (2010) studied the influence of airfoil leading edge thickness on far field sound pressure level. They show that an increase of leading edge thickness leads to the reduction of turbulent inflow noise. We propose here an empirical correction based on the data shown in Figure 6 of their publication. The reduction level in dB is calculated by linear interpolation based on the these data:

$$SPL_{reduction} (dB) = 9/50 \cdot (e/c)/(e/c)_{ref} \cdot f/U \cdot (\Lambda/c)_{ref}/(\Lambda/c) \quad (8)$$

where e is the airfoil maximum thickness, and Λ is the turbulent integral length scale. The subscription $_{ref}$ stands for the value of reference experimental data, which is: $(e/c)_{ref} = 0.12$, and $(\Lambda/c)_{ref} \approx 0.1$.

3.2 Adverse pressure gradient wall pressure model for trailing edge noise

In Amiet's trailing edge noise model, one of the most important input parameters is the spectrum of fluctuating wall pressure. An accurate estimation of this spectrum can be done with

direct numerical simulation (DNS) or large eddy simulation (LES), but it is really time and cost consuming. Amiet (1975), as a completion of his model, proposed an experiment based scaling formula, that is, by scaling the measured wall pressure spectrum with certain variables, all the spectra should collapse to a single curve. Later, Goody (2004) also proposed an improved wall pressure spectrum model that considers Reynolds effect. However, all these scaling models are based on zero gradient flow condition. For an airfoil, at trailing edge, it is often the case that an APG flow exists. Rozenberg *et al.*(2012) proposed a further improved model based on Goody's model, and takes into account the APG effect. He suggested that the wall pressure spectrum can be presented as:

$$\frac{\Phi_{pp}(\omega)U}{\tau_{max}^2 \delta^*} = \frac{[2.82\Delta^2(6.13\Delta^{-0.75} + F_1)^{A_1}] \left[4.2 \left(\frac{\Pi}{\Delta}\right) + 1\right] \tilde{\omega}^2}{[4.76\tilde{\omega}^{0.75} + F_1]^{A_1} + [8.8R_T^{-0.57}\tilde{\omega}]^{A_2}} \quad (9)$$

where the relevant parameters can be calculated as:

$$\tilde{\omega} = \frac{\omega \delta^*}{U}, \quad \tau_{max} = \max\left[\mu \frac{dU}{dy}\right], \quad \Delta = \frac{\delta}{\delta^*}, \quad \beta_c = \frac{\theta}{\tau_w} \frac{dp}{dx}, \quad A_1 = 3.7 + 1.5\beta_c, \quad R_T = \frac{\delta}{U} \frac{v}{u_\tau^2}$$

$A_2 = \min(3, 19/\sqrt{R_T})$, $F_1 = 4.76 \left(\frac{1.4}{\Delta}\right)^{0.75} [0.375A_1 - 1]$, with δ^* the boundary layer displacement thickness, δ the boundary layer thickness, θ the momentum thickness, τ_{max} the maximum wall shear stress along the airfoil surface, R_T the ratio of the outer to inner boundary layer time scale, and β_c the strength of the adverse pressure gradient.

The model is validated in the original paper of Rozenberg *et al.* (2012) against 5 different experimental results. In this paper, it is further validated against the data from DTU report (Bertagnolio, 2012). The experiments are launched in a wind tunnel with a symmetric airfoil NACA0015. Test velocities are 30 m/s, 40 m/s, 50 m/s, and the angle of attack is 0, 4, 8, and 12 degree. The chord length c is 0.9 m, and the microphone at which wall pressure is recorded is located at $x/c = 0.894$. Since no detailed boundary layer parameters are provided from the experiment, XFOIL is used to calculate the necessary input parameters for the APG model. For comparison, the test velocity of 30 m/s and 50 m/s at zero angle of attack case are considered. The comparison result is shown in Figure 2.

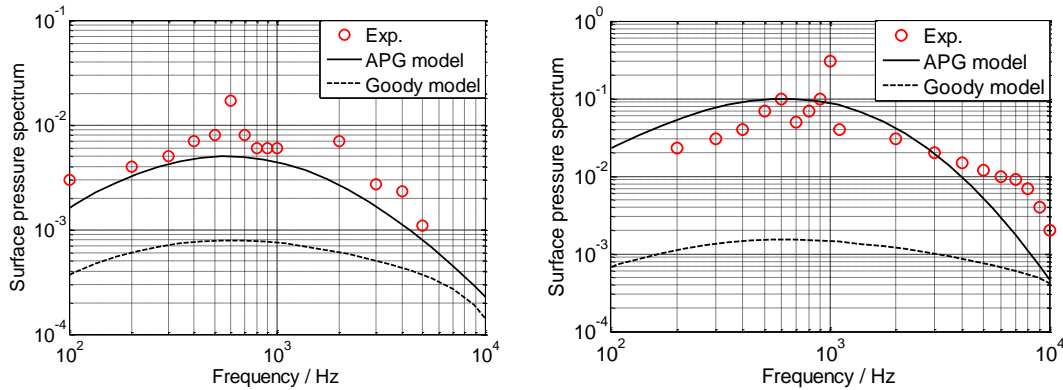


Fig. 2 Wall pressure spectrum measured by Bertagnolio (2012) (circles), and modeled by the APG model(solid line) and Goody's model(dashed line) respectively. Left, $U = 30\text{m/s}$; right, $U = 50\text{m/s}$.

4. Model validations against fixed airfoil measurements

4.1 Turbulent inflow noise validation

The model is compared to the experimental data from Paterson and Amiet (1976). Experiments are conducted in a wind tunnel using NACA0012 airfoil. The airfoil dimension is 0.23 m chord and 0.53 m span. The angle of attack is set to zero. The test velocities are 40, 60, 90, 120 and 165 m/s respectively, which corresponds to a free stream Mach number of approximately 0.12, 0.18, 0.27, 0.36, 0.5. The turbulence is generated by a bi-planar grid with a mesh size of 13.3 cm, the resulting turbulence intensity is of the order 4% ~5%, and the span-wise correlation length scale is around 3 cm. The noise is measured at 2.25 m radius from the

leading edge in the mid-span. Here the data from the microphone located directly above the leading edge are used.

The calculation results for various test velocities using large aspect ratio formulation are shown in Figure 3, with and without the leading edge thickness correction. The correction is most necessary for low Mach number at higher frequency range.

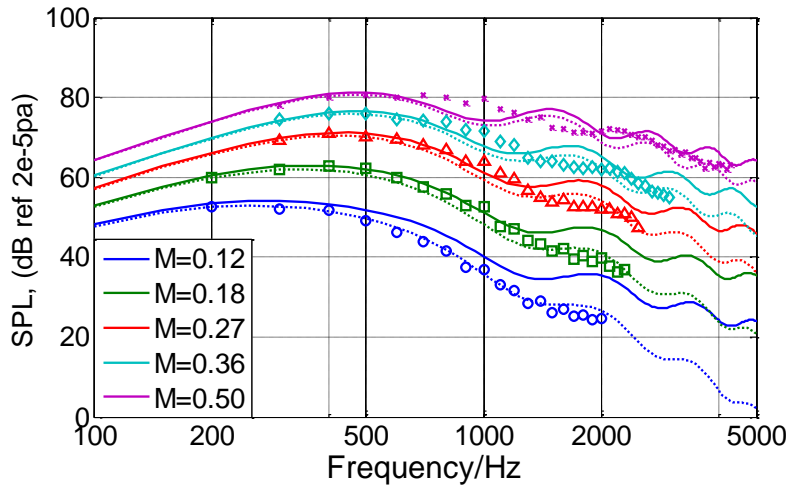


Fig. 3 SPL of turbulent inflow noise. Symbols: measurement from Paterson and Amiet (1976); solid line: without thickness correction; dashed line: with thickness correction.

4.2 Trailing edge noise validation

For the validation of trailing edge noise, the experimental data from Brooks and Hodgson (1981) are considered. The test airfoil is again NACA 0012, with a chord of 0.61 m and a span of 0.46 m. The test velocity chosen for the current validation is 69.5 m/s, and the angle of attack is zero. The reference location is 1.8 cm upstream of the trailing edge and the receiver is located 1.22 m away directly above the trailing edge in the mid-span. The span-wise correlation length $\ell_y(\omega)$ that is needed for Equation (6) and (7) is determined by Corcos's model (Moreau and Roger, 2005):

$$l_y(\omega) = \frac{bU_c}{\omega}$$

with $b = 1.47$ being an experimental constant, and $U_c = 0.75U$ being the convective velocity.

The results for wall pressure spectrum and far field SPL are shown in Figure 4. The results from Goody's wall pressure spectrum model is also plotted for comparison with the APG model. Again we can see that the adverse pressure gradient tends to increase the far field SPL, and that the APG model provides better results than Goody's model.

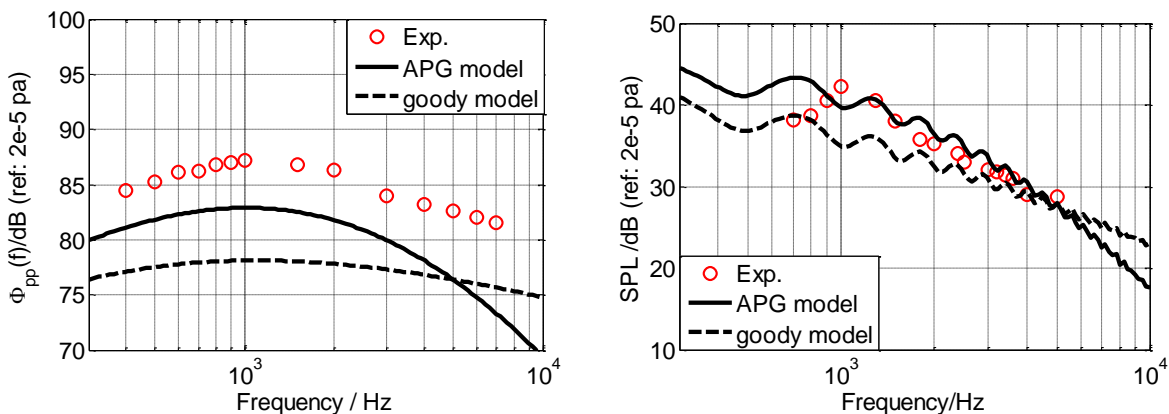


Fig. 4 Comparison between APG model and Goody's model against experiment. Left: wall pressure spectrum comparison; right, far field SPL comparison.

5. Results and comparison against full size wind turbine measurements

5.1 Exact formulation and sub-critical gust effect

In section 2.1, the power spectral density S_{pp} is simplified under the assumption of large aspect ratio. For the calculation of a wind turbine, since each blade is cut in segments on which the noise models are applied individually, it is not guaranteed that this assumption is valid for all the segments. Thus it is necessary to examine the validity of the large aspect ratio approximation for a wind turbine.

A first test on "segment aspect ratio" is carried out with a fixed NACA0012 airfoil. The chord is set to 0.5 m, and the span is set to 0.25 m, 0.5 m, 1.5 m and 2.5 m respectively, Mach number is 0.2. The observer is located in the mid-span plane 2 m above the airfoil. The results for trailing edge noise are shown in Figure 5, from which we can see that when the aspect ratio is more than 3, the simplified formula provides really close results compared to those from the exact formula. When the aspect ratio is less than 3, the main discrepancy between the two appears for frequency less than 600Hz.

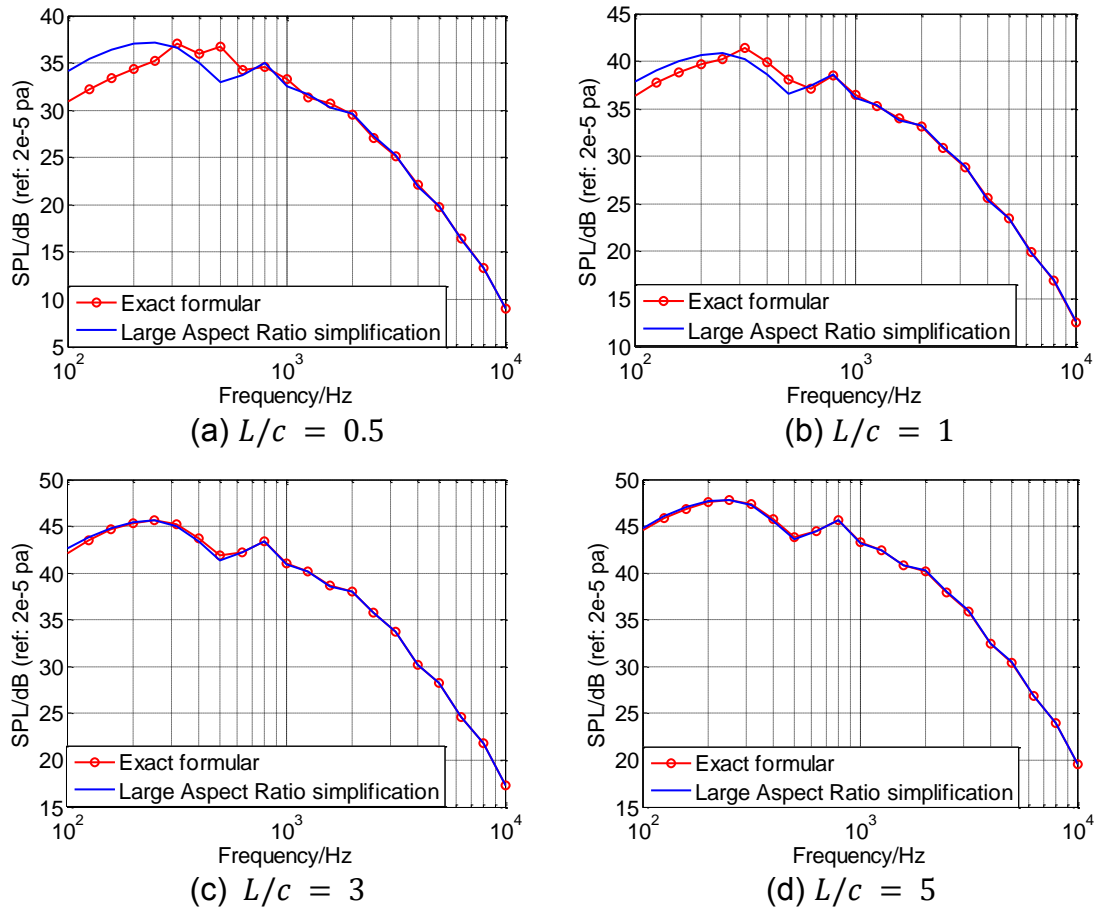


Fig.5 Trailing edge SPL calculated by the exact and simplified formula for difference aspect ratio respectively.

The integration over \bar{K}_y in Equation (6) involves dealing with sub-critical gusts, that exists when $\bar{\kappa}^2 = \bar{\mu}^2 - \bar{K}_y^2/\beta^2 < 0$. A set of plots of with respect to airfoil response function \mathcal{L} with respect to \bar{K}_y are shown in Figure 6. The parameters are: chord $c = 0.13$ m, span $L = 0.13$ m, Mach number $M = 0.05$ and 0.3 respectively, the test frequency is 1000 Hz. The angles indicated in the figures are the observer angles in the mid-span plane, where 0° means downstream in the airfoil plane and 90° means in direction normal to the airfoil. We observe that the airfoil response function decreases rapidly for subcritical cases when the normalized span-wise wave number increased. However, gusts with \bar{K}_y close to unity can have a significant effect on the final results.

To understand the importance of the subcritical gusts for different frequencies, the *SPL* due to all the super-critical gusts and all the sub-critical gusts respectively, as well as the sum of the two are plotted in Figure 7. We can see that the sub-critical gusts are dominant at low frequency (up to 100Hz), and decrease very fast at higher frequency range. Since for the aspect ratio of 1, the simplified formula could provide satisfying results for most of audible frequency range (200Hz and above), it will be used to calculate wind turbine noise in the next section, even though the sub-critical gusts are neglected consequently.

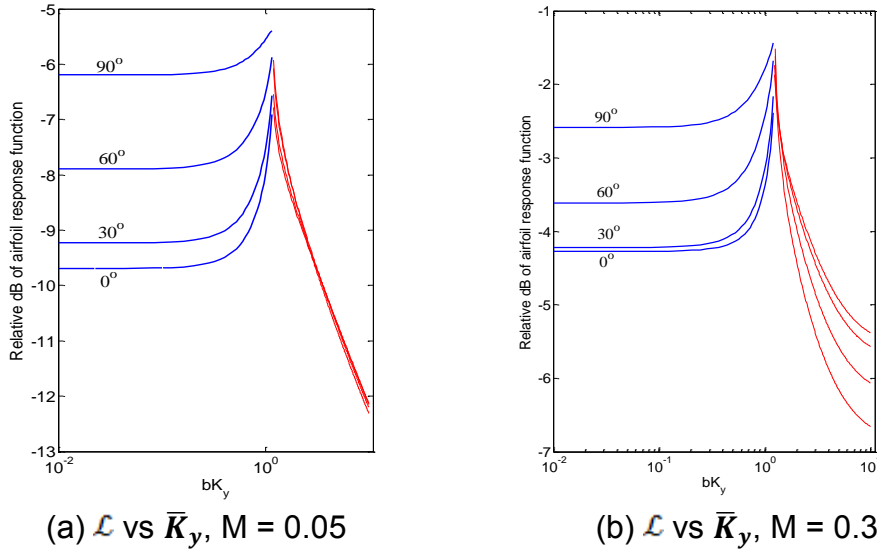


Fig.6 Airfoil response function \mathcal{L} as a function of \bar{K}_y and far field trailing edge noise. Blue line: super-critical gust, red line: sub-critical gust.

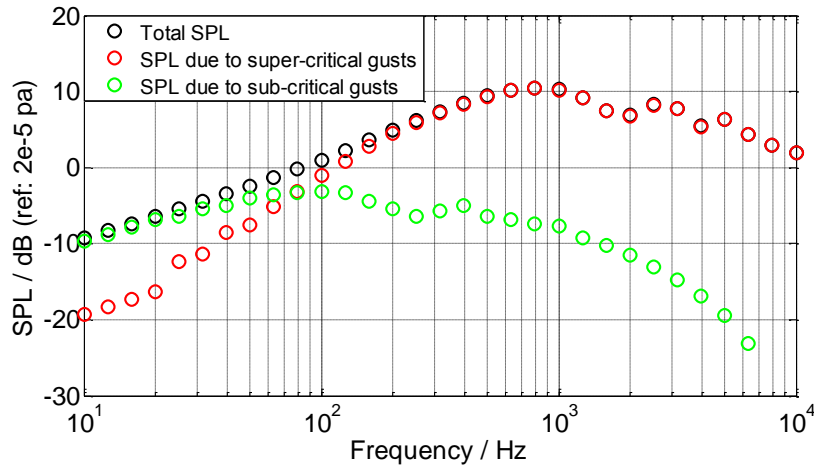


Fig.7 SPL of trailing edge noise due to super and sub-critical gusts, $M = 0.3$, chord $c = 0.13\text{m}$, span $L = 0.13$. Observer in the mid-span 2m above the airfoil.

Doppler effect due to blade rotation is taken into account by relating the PSD of a moving source to a fixed source at the same instant location (Schlinker *et al*, 1981):

$$S_{pp}^m(\omega) = \frac{1}{Dopp} S_{pp}^f(\omega')$$

where $Dopp$ is the Doppler factor defined by $Dopp = \frac{\omega'}{\omega}$, ω is the source frequency and ω' is the observer measured frequency.

5.2 Application on a wind turbine and validation against measurements

The comparison is made for a Bonus 300kW wind turbine using data from Zhu *et al* (2005). The main parameters for this type of wind turbine and meteorology conditions are given in Table 1.

Table 1 Bonus 300kW wind turbine main parameters

Rotor radius	Tower Height	Rotor angular speed	Airfoil profile	Chord length	Wind speed (10m height)	Observer location	Ground roughness
15.5 m	31m	3.7 rad/s	NACA 632xx	0.5m-1.5m	8 m/s	40m down wind	30mm

Wind shear effect is considered in the calculation by taking an experimental log law relation:

$$U_i = U_{ref} \left(\frac{H_i}{H_{ref}} \right)^\gamma$$

where U_i is the velocity at height H_i , U_{ref} is the reference velocity at reference height H_{ref} , taken as the hub height here, and (Zhu *et al.* 2005)

$$\gamma = 0.24 + 0.096 \log_{10} z_0 + 0.016(\log_{10} z_0)^2 \quad (10)$$

z_0 is the ground roughness. The turbulence intensity I and turbulence integral length scale Λ are calculated by the relations given in Zhu (2005), as:

$$I = \gamma \cdot \frac{\log_{10} \frac{30}{z_0}}{\log_{10} \frac{z}{z_0}}, \quad \text{and} \quad \Lambda = 25 \cdot z^{0.35} z_0^{-0.063},$$

where γ is the same as defined in Equation 10. The turbulence energy spectrum is calculated using the isotropic Von Kármán spectrum. Plot of the energy spectrum for integral length scale $\Lambda = 100$ m with various turbulence intensities and a turbulence intensity $I = 0.1$ with various integral length scales are shown in Figure 8.

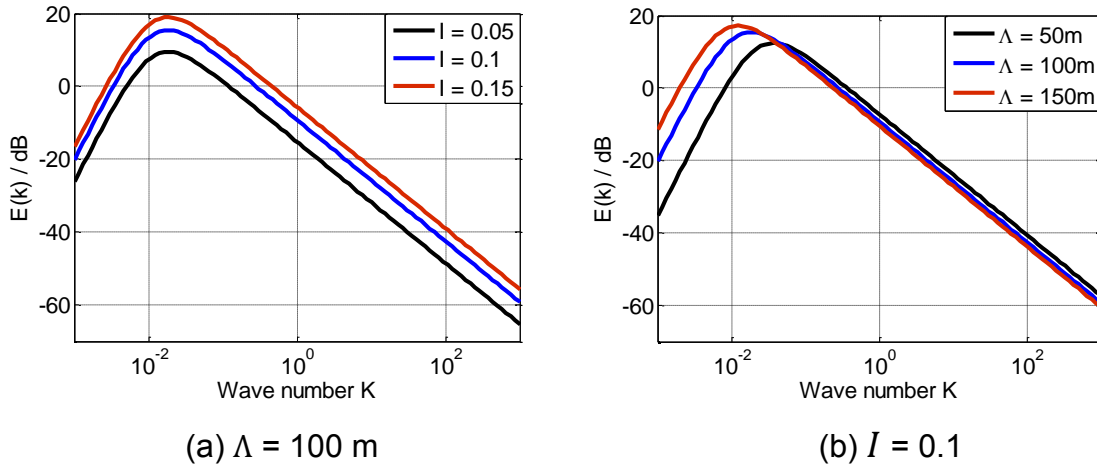


Fig. 8 Von Kármán turbulence energy spectra for different integral length scales and turbulence intensities.

The calculation procedures are the following: first, each wind turbine blade are artificially cut in several segments, here, 10 segments of 1.5m length for each blade, so that the maximum aspect ratio remains no larger than 1. According to the flow conditions at each segment, the boundary layer parameters required by the APG wall pressure model are calculated by XFOIL (version 6.96) and stored in advance. The noise models for turbulent inflow noise and trailing edge noise are then applied for each segment, with thickness correction and Doppler effect considered. The final total noise perceived by the observer is obtained by logarithm summation over all the segments.

Figure 9 shows the sound power level from the calculation compared to the measurement. The results are shown in 1/3-octave bands, A-weighted and averaged over one rotating period. It is needed to say that the measured data includes all the noise mechanisms (stall noise, trailing edge bluntness noise, etc) which are not considered by the models. According to our model, trailing edge noise is dominant over turbulent inflow noise for this type of wind turbine under these meteorological conditions. The agreement between the calculation and the measurement

is acceptable in the frequency range of 600 Hz to 8000 Hz, but at lower frequency range, the results shows up to 20 dB differences. Turbulent inflow noise level is rather low, which might be due to the large turbulent integral length scale, that ranges between 120 m to 180 m. On the right figure, it is shown that a decrease of turbulent integral length scale will increase the noise level for a fixed turbulence intensity.

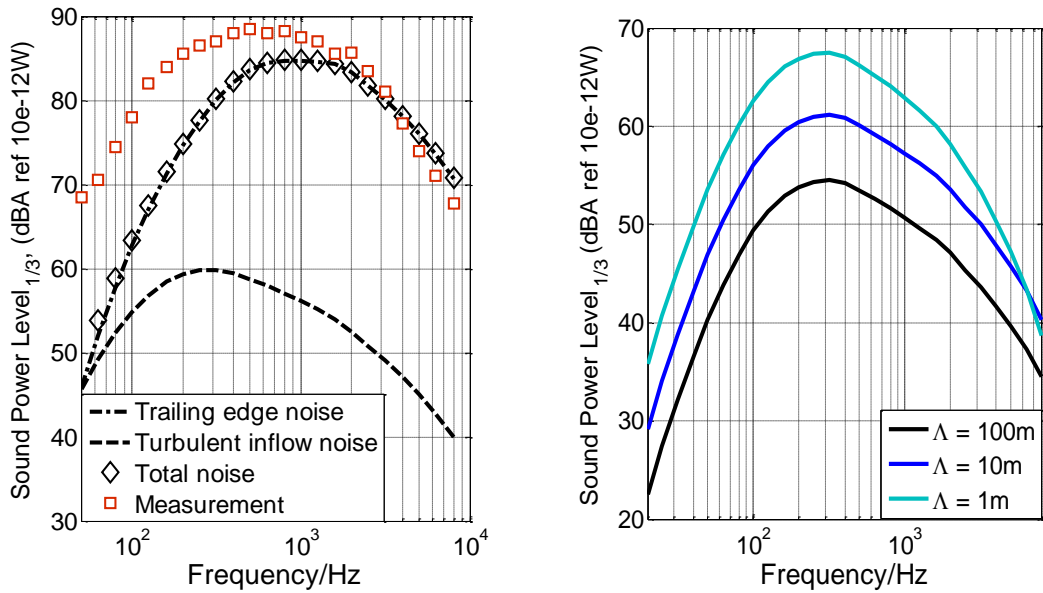


Fig. 9 Left: Comparison of turbulent inflow noise and trailing edge noise models against measurement. Right: influence of turbulent integral length scale on the turbulent inflow noise.

The comparison for trailing edge noise using APG wall pressure model and Goody's wall pressure model is shown in Figure 10. The results are shown in 1/3-octave bands. It is clear that an adverse pressure flow condition greatly increases the trailing edge noise. By using APG model, the results are much closer to the measurements. Figure 11 shows the thickness correction for turbulent inflow noise. Under this atmospheric turbulence condition, more precisely, when the turbulent integral length scale is much larger than the size of blade chord, this correction is not significant.

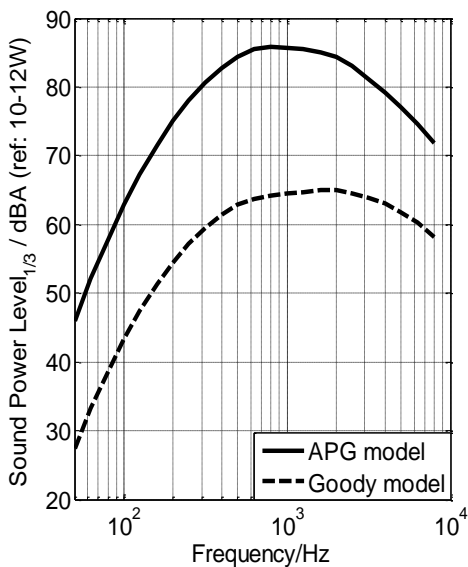


Fig.10 Comparison between APG model and Goody model for trailing edge noise.

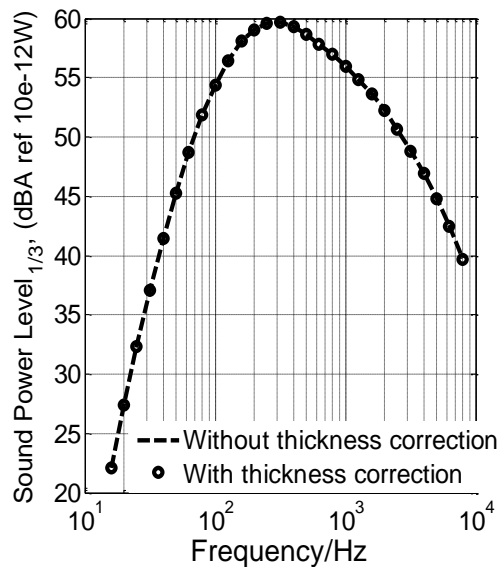


Fig.11 Turbulent inflow noise with/without leading edge thickness correction.

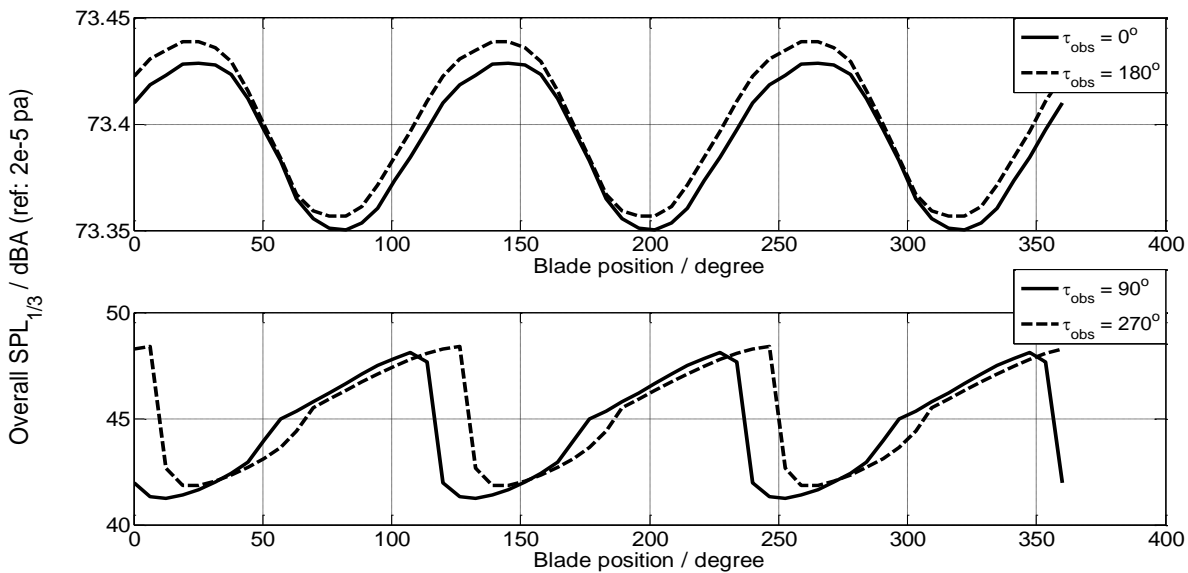


Fig.12 Total SPL variation during one period perceived at difference observer location. $\tau_{obs} = 0^\circ$ corresponds to the observer at downwind direction, and $\tau_{obs} = 90^\circ$ corresponds to the observer at rotor plane on the left side when facing downwind direction.

Figure 12 shows the total SPL variation during one rotating period, the observer is at a 40 m distance from the wind turbine. From the result we can see that when the observer is upwind or downwind direction (corresponds to $\tau_{obs} = 0^\circ$ and $\tau_{obs} = 180^\circ$), the perceived SPL is almost constant; but for an observer located in the rotor plane direction (corresponds to $\tau_{obs} = 90^\circ$ and $\tau_{obs} = 270^\circ$), even though the overall SPL is much less, but the variation during one period reaches up to 6 dB. These trends agree with the results from Lee *et al*(2013).

The directional feature of overall SPL averaged over one rotating period is shown in Figure 13. The wind is coming from the left to the right. The pattern shows a dipole shape, as was shown in many previous work (Zhu 2005, Lee *et al*, 2013), with a bit lower level in the rotor plane direction, and a higher level in the wind direction.

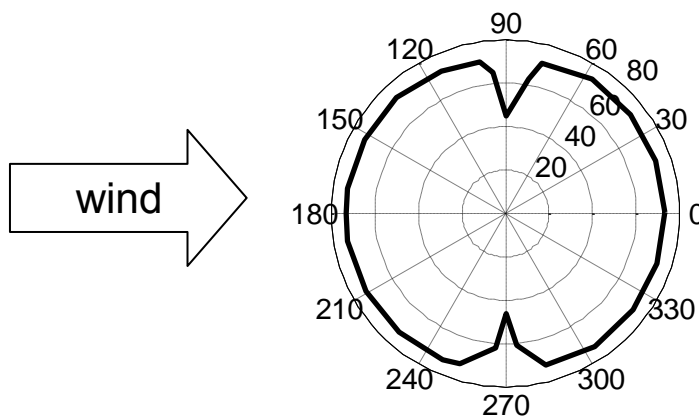


Figure 13 Directivity of overall SPL in dB(A).

6. Conclusions

Amiet's analytical model for turbulent inflow noise and trailing edge noise are extended by considering an APG wall pressure model and a leading edge thickness correction respectively. The extended models are first validated against fixed airfoil measurements, then applied to a full size wind turbine. APG wall pressure model greatly improved the accuracy for trailing edge

noise prediction, while for the turbulent inflow noise, the thickness correction does not seem significant when the atmospheric turbulent length scale is very large. The results of total SPL as a function of blade position are expected to give an explanation for the 'swish' effect. When the observer is located at rotor plane direction, the amplitude modulation causes a strong 'swish'; while if the observer is located at upwind or downwind direction, the effect is hardly noticeable. In the future, the model will need to be compared to a more detailed wind turbine experimental campaign, since the comparison with data from the literature is not completely satisfying. Also, the model will be coupled to a propagation model and a more realistic model of the atmospheric boundary layer will be considered. Finally, other noise mechanisms that can give rise to rapid time fluctuations such as stall noise will be investigated.

Acknowledgements

The authors would like to thank Michel Roger and Yannick Rozenberg from the Laboratoire de Mécanique des Fluides et d'Acoustique (LMFA) of the Ecole Centrale de Lyon for useful discussions regarding Amiet's theory.

References

- Amiet R.K (1975) *Acoustic radiation from an airfoil in a turbulent stream*, Journal of Sound and vibration 41(4), 407-420
- Amiet R.K (1976) *Noise due to turbulent flow past a trailing edge*, Journal of Sound and Vibration 47(3), 387-393
- Bertagnolio (2012) *Low noise airfoil-Final report*, EUDP project
- Brooks T.F and Hodgson T.H (1981) *Trailing edge noise prediction from measured surface pressures*, Journal of Sound and Vibration 78(1), 69-117
- Brooks T.F, Pope D.S and Marcolini M.A (1989) *Airfoil self-noise and prediction*, NASA reference publication 1218
- Goody M (2004) *Empirical spectral model of surface pressure fluctuations*, AIAA Journal 42(9) 1788-1794
- Howe M.S(1978) *A review of the theory of trailing edge noise*, NASA Contractor report 3021
- Lee S, Lee S and Lee S (2013) *Numerical modelling of wind turbine aerodynamic noise in the time domain*, Journal of Acoustical Society of America, 133(2)
- Moreau S and Roger M (2005) *Effect of airfoil aerodynamic loading on trailing-edge noise sources*, AIAA Journal, 43(1)
- Oerlemans S, Sijtsma P, Lopez B.M (2007) *Location and quantification of noise sources on a wind turbine*, Journal of Sound and Vibration, 299
- Paterson R.W and Amiet R.K (1976) *Acoustic radiation and surface pressure characteristics of an airfoil due to incident turbulence*, NASA report CR-2733

Rozenberg Y (2007) *Modélisation analytique du bruit aérodynamique à large bande des machines tournantes: utilisation de calculs moyennés de mécanique des fluides*. PhD thesis, L'école centrale de Lyon.

Rozenberg Y, Robert G, Moreau S (2012) *Wall-pressure spectral model including the adverse pressure gradient effects*, AIAA Journal 50(10)

Roger M and Moreau S (2005) *Back-scattering correction and further extensions of Amiet's trailing-edge noise model. Part 1: theory*, Journal of Sound and Vibration, 286, 447-506

Roger M and Moreau S (2010) *Extensions and limitations of analytical airfoil broadband noise models*, International Journal of Acoustics 9(3), 273-305

Schlinder R.H and Amiet R.K (1981) *Helicopter Rotor Trailing Edge Noise*, NASA Contractor Report 3470.

Styles P, Westwood R.F, Toon S.M, Buchingham M.P, Marmo B, Carruthers B (2011) *Monitoring and mitigation of low frequency noise from wind turbines to protect comprehensive test ban seismic monitoring stations*, 4th International Meeting on Wind Turbine Noise, Rome, Italy

Zhu W J, Heilskov N, Shen W.Z, Sorensen J.N (2005) *Modelling of aerodynamically generated noise from wind turbines*, Journal of Solar Energy Engineering Vol.127